ALEPH 94-043
PHYSIC 94-039
F. Saadi et al.
15.03.1994

A precise measurement of the partial width ratio $R_b = \Gamma_{Z\to b\bar{b}}/\Gamma_{Z\to hadrons}$ using hemisphere Double Tag methods

F. Saadi, A. Falvard, P. Henrard, S. Monteil, P. Perret

University Blaise Pascal - Clermont II/In2P3

March 2. 1994

Abstract

We present a set of measurements for the ratio $R_b = \Gamma_{Z\to b\bar{b}}/\Gamma_{Z\to hadrons}$ using hemisphere Double Tag methods with three different b-taggers : high $p_\perp$ leptons, event shape variables and lifetime tag. Using data collected up to 1992, our combined result is : $R_b = [22.27 \pm 0.23(stat.) \pm 0.27(syst.)]\%$ being a 1.6% measurement. The error due to the uncertainty on the partial width ratio R_c is $\pm 0.07\%$. This result is mainly based on the large mass of the b quark, and hence is for a large part uncorrelated with the published result of ALEPH using only a lifetime tag.

1 Introduction

In this note, we describe a set of measurements of R_b mainly based on the large mass of the b quark, the aim being to show that we can obtain a precision measurement of R_b which is uncorrelated with the published result of ALEPH based only on a lifetime tag [1]. All the details on this work can be found in ref. [2].

By using the three different b-taggers :

- High $p_\perp$ leptons,
- Event shape variables,
- Lifetime tag,

we have developed four Double Tag methods :

1. Method (1) : Single and double tagged events by high $p_\perp$ leptons.
2. Method (2) : Event shape and high $p_\perp$ leptons.
3. Method (3) : Event shape and lifetime tag.
4. Method (4) : Lifetime tag and high $p_\perp$ leptons.

The method (1) has been already published with the '90 and '91 data [3] and presented at Marseille last year for the '92 data [4]. So, we will only concentrate on a preliminary study of background events and on the result obtained for R_b with the data collected in 1992. More details can be found in ref. [2] and [5].

The method (2) is also published with the '90 and '91 data [6] and a very detailed description of the method and of the systematic errors can be found in [2] and [7]. So, we will perform as for method (1).

The methods (3) and (4) are new and they will be discussed in more details in this paper.

For each analysis, the hadronic events are split into two hemispheres with respect to the thrust axis (defined with energy flow tracks), and the b taggers are applied to each hemisphere separately.

2 Method (1) : Single and double tagged events with high $p_\perp$ leptons

2.1 Principle of the method

This method uses both single and double tagged hadronic events with leptons to eliminate the uncertainties on the details of b decays (semileptonic branching ratios, modelling, etc) and fragmentation. The two sample of events are defined in the following way :

1. Single tagged sample N_{st} : events in which one and only one hemisphere contains at least one high $p_\perp$ lepton ;

2. Double tagged sample N_{dt} : events in which both hemispheres contain at least one high $p_\perp$ lepton.

From these two samples, $R_b^{(1)}$ is derived by solving the following system of two equations with two unknowns N_b and ϵ_b :

$$\begin{array}{rcl} N_{st} & = & 2\epsilon_b(1-C\epsilon_b)N_b \; + \; N_{st}^{udsc} \\ N_{dt} & = & C\epsilon_b^2 N_b \; + \; N_{dt}^{udsc} \end{array} \qquad (1)$$

• N_b is the number of $Z \rightarrow b\bar{b}$ events in the hadronic sample after the CLAS 16 selection. Since the efficiency of the CLAS 16 selection is different between b and non-b events (higher for b events), a correction factor C_b is introduced to obtain R_b from N_b; we have : $R_b^{(1)} = C_b N_b / N_{had}$. C_b has been determined from Monte Carlo and is equal to 0.992 ± 0.008 where the error is due to the number of simulated events used.

• ϵ_b is the probability to tag one hemisphere of a $b\bar{b}$ event by a high $p_\perp$ lepton. It contains all the uncertainties related to decay modelling, fragmentation and branching ratios of the b.

• N_{st}^{udsc} and N_{dt}^{udsc} are the number of single and double tagged light quark events. They are estimated from Monte Carlo. Since the tagging efficiency is different for $c\bar{c}$ and uds events, the determination of these numbers depends on the charm physics parameters like the charm fragmentation, R_c, the branching ratio of $c \rightarrow l$ and the modelling of the $c \rightarrow l$ momentum spectrum.

• C is defined as $\epsilon_{b\bar{b}}/\epsilon_b^2$ where $\epsilon_{b\bar{b}}$ is the probability to tag the two hemispheres of a $Z \rightarrow b\bar{b}$ event. It accounts for possible correlations between the tagging efficiencies of the two hemispheres like geometrical acceptance effects which can modify the ratio of double over single tagged events. It has been estimated from Monte Carlo by using 265,000 fully simulated $Z \rightarrow b\bar{b}$ events. Its value $C = 1.002 \pm 0.012$ is consistent with one. We have checked that the value of C was stable for different cuts on the azimutal angle ϕ (see fig. 1) and on the polar angle of the thrust axis.

We have also verified that C does not depend on the $p_\perp$ cut and hence is independent of the physical origin of the leptons, and that the values obtained for different versions of the simulation corresponding to different years of data taking are compatible within the statistical error.

2.2 Results

This method has been applied to 131,740, 248,863 and 653,938 hadronic events selected respectively in 1990, 1991 and 1992 with $|\cos\theta_{thrust}| < .9$. The number

	'90 data			
$p_\perp^{cut}$	0.75	1.00	1.25	1.50
N_{st}^e	3761	2921	2272	1770
N_{st}^μ	5598	4274	3319	2552
N_{st}	8782	6813	5376	4179
N_{dt}^e	104	75	48	37
N_{dt}^μ	190	123	82	41
N_{dt}	534	369	232	144

	'91 data			
$p_\perp^{cut}$	0.75	1.00	1.25	1.50
N_{st}^e	7519	5834	4525	3504
N_{st}^μ	11608	8841	6857	5319
N_{st}	17812	13839	10865	8486
N_{dt}^e	185	76	67	40
N_{dt}^μ	409	263	176	107
N_{dt}	1132	734	478	296

	'92 data				
$p_\perp^{cut}$	0.75	1.00	1.25	1.50	1.75
N_{st}^e	19579	15129	11665	8901	6593
N_{st}^μ	31412	23974	18590	14368	11067
N_{st}	47580	36919	28886	22468	17211
N_{dt}^e	470	310	197	108	64
N_{dt}^μ	1047	710	472	308	172
N_{dt}	2947	1973	1281	784	447

Table 1: Number of single and double tagged events for electrons N_{st}^e (N_{dt}^e), muons N_{st}^μ (N_{dt}^μ) and for both electrons and muons N_{st} (N_{dt}). Note that the events N_{st}^e et N_{st}^μ can a priori contain muons and electrons, and so the sum of these two numbers can be greater than N_{st}. $p_\perp$ is in units of GeV/c.

	'92 data			'91 data			'90 data		
N_{lep}	0 tag	1 tag	2 tag	0 tag	1 tag	2 tag	0 tag	1 tag	2 tag
1	94185	22355		35867	8426		18220	4242	
2	9460	5845	1038	351	2198	405	1717	1013	201
3	662	653	232	230	220	65	113	109	30
4	42	33	11	10	21	8	2	12	1
Total	104349	28886	1281	39648	10865	478	20052	5376	232

Table 2: Origin of the single and double tagged events for $p_\perp \geq 1.25$ GeV/c. "0 tag" are the events with no tagged lepton.

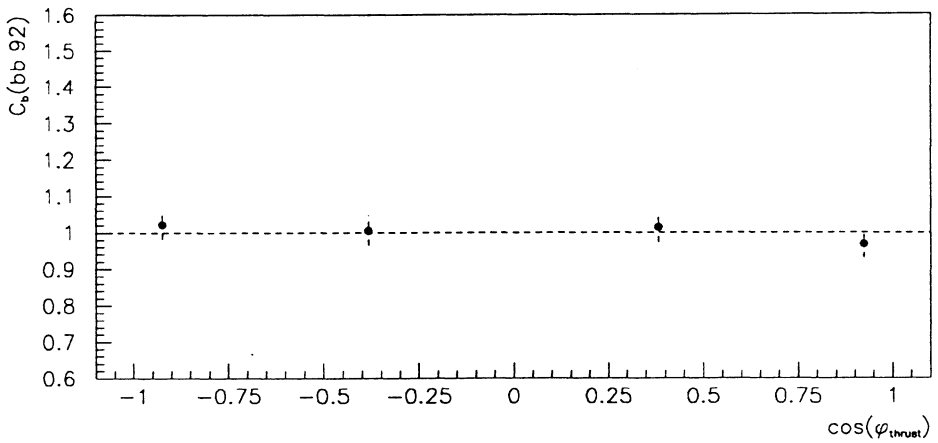

Figure 1: Value of the C factor with the azimutal ϕ angle of the thrust axis for $Z \rightarrow b\bar{b}$ events simulated with the '92 geometry of the detector.

of the single and double tagged events for the different years of data taking are summarized in tables 1 and 2.

The values of R_b and ϵ_b obtained for $p_\perp > 1.25$ GeV/c (value which gives the smallest overall error with the present statistics) are given in tables 3 and 4. The same analysis has been done for several cuts on the lepton transverse momentum ; the results are illustrated on figure 2.

	'92 data		'91 data		'90 data	
	$R_b^{(1)}$ (%)	ϵ_b (%)	$R_b^{(1)}$ (%)	ϵ_b (%)	$R_b^{(1)}$ (%)	ϵ_b (%)
e	23.51 ± 1.70	3.54 ± 0.25	23.18 ± 2.50	3.67 ± 0.40	18.43 ± 2.60	4.42 ± 0.60
μ	22.56 ± 1.00	5.56 ± 0.30	21.17 ± 1.53	5.75 ± 0.40	20.22 ± 2.00	5.49 ± 0.60
l	22.53 ± 0.60	9.21 ± 0.24	22.32 ± 0.97	9.21 ± 0.39	21.21 ± 1.30	9.01 ± 0.54

Table 3: Values of $R_b^{(1)}$ and of ϵ_b obtained with the data of 1990, 1991 and 1992 for the electrons (i.e. double tagged events with di-electrons ee), the muons (i.e. double tagged events with di-muons $\mu\mu$) and for leptons (double tagged events including ee, $\mu\mu$ and $e\mu$). So, the value of R_b^l is not simply the weighted average of R_b^e and R_b^μ.

The figures 2 and 3 and the tables 3 and 4 show that the value of $R_b^{(1)}$ has no $p_\perp$ dependence within the statistical errors for both electrons and muons, (even if the value at 1.75 GeV/c is higher due to a possible fluctuation in the muon sample) and is compatible within the statistical errors between electrons and muons and between the different years of data taking.

	Data '90+'91+'92	
	$R_b^{(1)}$ (%)	ϵ_b (%)
e	22.70 $\pm$ 1.30	3.70 $\pm$ 0.20
μ	21.90 $\pm$ 0.80	5.60 $\pm$ 0.20
l	22.30 $\pm$ 0.48	9.20 $\pm$ 0.20

Table 4: Values of $R_b^{(1)}$ and ϵ_b obtained with the data taken up to 1992 for electrons, muons and leptons. Same remark as for the previous table.

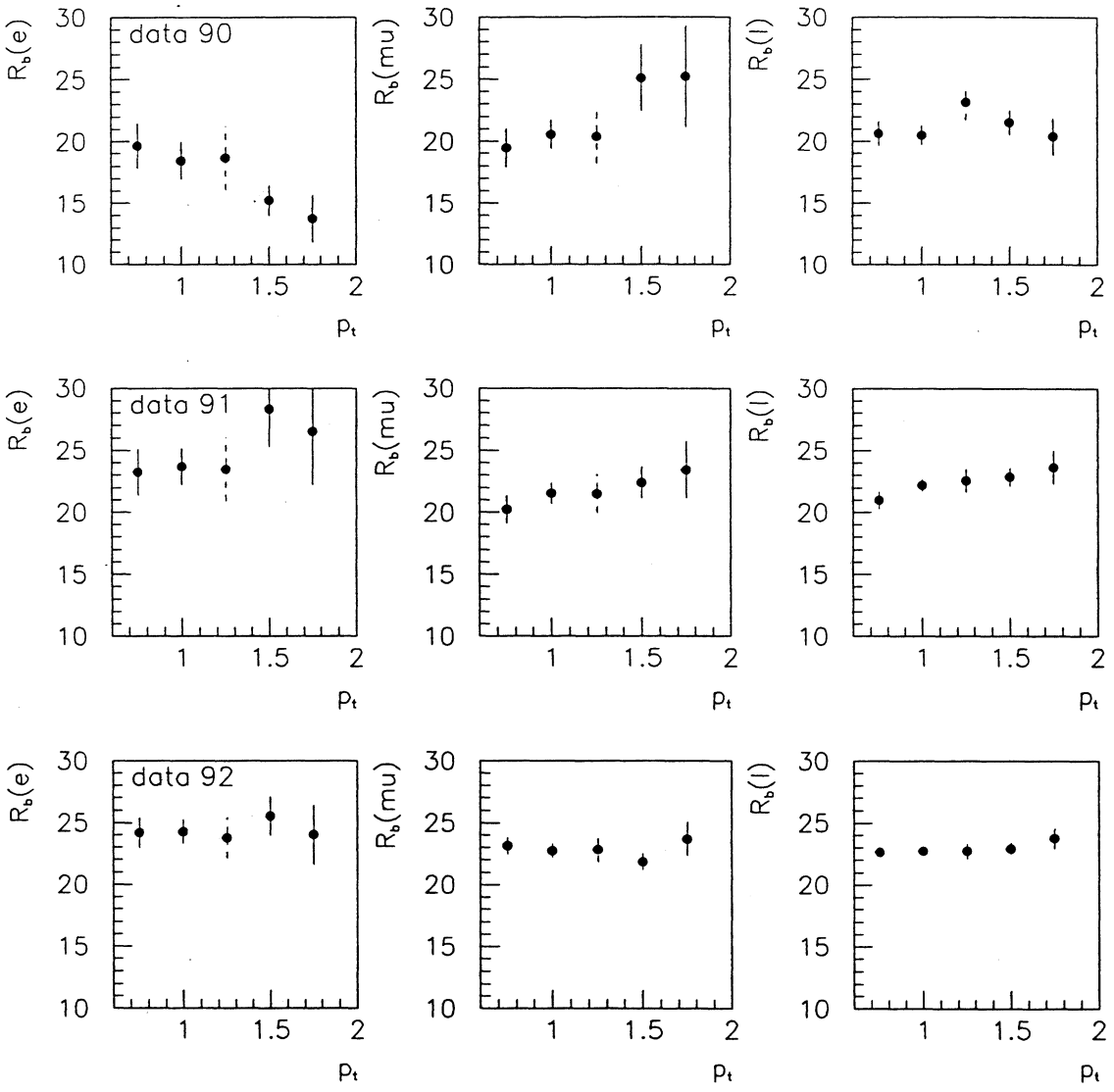

Figure 2: Values of $R_b^{(1)}$ for different $p_\perp$ cuts obtained with electrons ($R_b(e)$), muons ($R_b(\mu)$) and with both electrons and muons ($R_b(l)$) for the data collected in 1990, 1991 and 1992. Uncorrelated statistical errors are shown except for 1.25 GeV/c where the full statistical error is plotted.

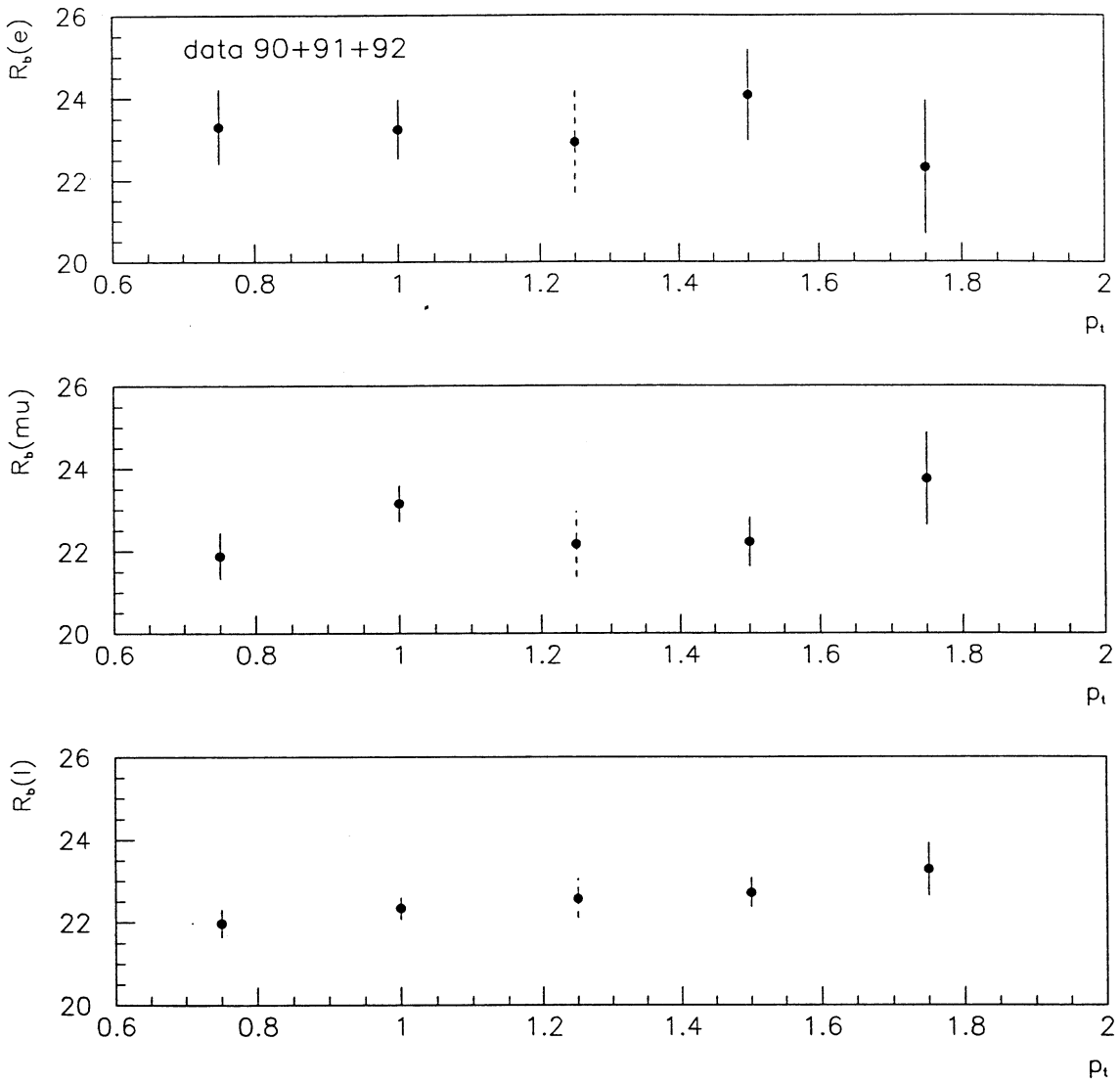

Figure 3: Values of $R_b^{(1)}$ for '90+'91+'92 data as function of the $p_\perp$ cut : a) for electrons, b) for muons and c) for both electrons and muons. Uncorrelated statistical errors are shown except for 1.25 GeV/c where the full statistical error is plotted.

2.3 Systematic errors

The sources of systematic errors have two origins :

- *The charm physics*

The only change compared to the published result (where only the DELCO data were used) is the systematic coming from the $c \rightarrow l$ modelling which is now estimated by using the MARKIII and DELCO data to determine the values of the two parameters p_F and m_s of the Altarelli model according to the prescriptions of the Heavy Flavour Electroweak working group [8]. They obtain $p_F = 0.467^{+0.205}_{-0.114}$ GeV/c and $m_s = 0.001 \pm 0.152$ GeV/c^2. The resulting momentum distribution is harder than in our standard Monte Carlo (as a consequence, this increases the number of charm events in the region above 1.25 GeV/c).

It has been shown in [8] that a very good estimate of the systematic error due to the modelling of $c \rightarrow l$ transitions can be obtained by simply varying p_F within 1σ with m_s fixed at 0.001 GeV/c^2. The corresponding systematic error on $R_b^{(1)}$ is given in table 5.

- *The lepton identification efficiency and the contamination from hadrons*

Since N_{st}^{udsc} and N_{dt}^{udsc} are taken from the simulation, we have to check carefully the simulation of background events. Two points are of first importance : the determination of the lepton identification efficiency and of the hadron misidentification probability, and the shape of the $p_\perp$ distribution of the background.

The lepton identification efficiency and the hadron misidentification probabilities are determined directly from the data and correction factors from CALPOIDS are applied to the Monte Carlo for each year of data taking [11].

However, the shape of the $p_\perp$ distribution of the background has not yet been studied in details. In this note, we only want to show some preliminary plots on this problem. A forthcoming ALEPH note will be produced on this subject.

– Electron

The shape of the $p_\perp$ distribution for the electrons from conversions in the detector material can be compared directly between data and Monte Carlo thanks to the high purity in electron of the sample selected by requiring that the materialisation point be in a part of the detector which has a high density of material : the VDET, the walls of the ITC or the inner wall of the TPC [11]. Figure 4 shows the $p_\perp$ distribution for '92 data and '92 Monte Carlo. No disagreement is seen at high $p_\perp$ but the statistics is limited.

– Muon

For the muons, the situation is not so good since it is not easy to control both the normalisation and the shape of the $p_\perp$ distribution of the muon background directly from the data, and since the background is important even in the high $p_\perp$ region (see table 10).

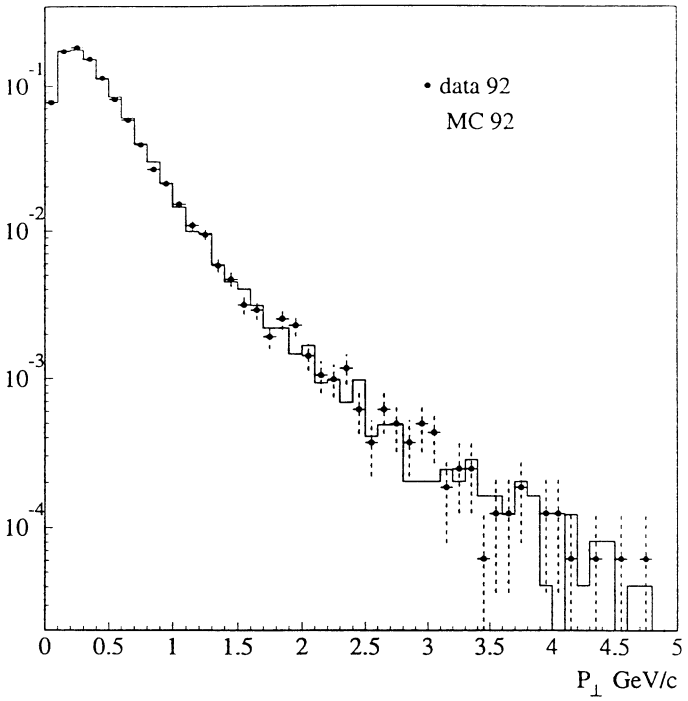

Figure 4: Transverse momentum distribution of electron candidates from conversions for '92 data (points) and '92 Monte Carlo (histogram). The two contributions are normalized to the same area.

For the muons produced in K and π decays, we have no control from the data and so we have to rely on Monte Carlo for both the rate and the shape of the $p_\perp$ distribution. A $\pm 10\%$ uncertainty is usually assigned on this contribution for all the analyses using high $p_\perp$ leptons (mixing, asymmetry, etc). A possible method to enrich a sample in muons from decays is to select muon candidates with large d_0 values. According to the Monte Carlo and with the muon identification algorithms, we can select a sample with 70% of decays with the cut $|d_0| > 0.2$ cm. Figure 5 shows the $p_\perp$ distribution of this enriched sample. For $p_\perp > 1.25$ GeV/c, we obtain : $N_{data}/N_{MC} = 0.8 \pm 0.3_{stat.}$ So, the statistics is too small to conclude.

For the punch-through, we can measure the misidentification probability from the data by selecting pure samples of pions from $Z \rightarrow \tau^+\tau^-$ events with $\tau^+ \rightarrow \rho^+\nu_\tau$ and $\rho^+ \rightarrow \pi^+\pi^0$, and from $K^0_s \rightarrow \pi^+\pi^-$. The correction factor applied to the Monte Carlo is : $R^\mu_{misid} = 1.16 \pm 0.21_{stat.} \pm 0.09_{syst.}$ with the '90+'91 data and $R^\mu_{misid} = 1.19 \pm 0.13_{stat.} \pm 0.12_{syst.}$ with the '92 data. where the systematic error comes from the subtraction of the μ-decays contribution. However, we have not enough statistics to determine accurately this number at high $p_\perp$. For instance for $p_\perp > 1.25$ GeV/c, we find : $R^\mu_{misid} = 0.93 \pm 0.60(stat.)$ with the '92 data.

The shape of the background contribution can be studied by looking at the $p_\perp$ distribution of all the charged tracks in the hadronic Z events (see fig. 6) and of the $\pi^\pm$ coming from K^0_s (see fig. 7). We see that the $p_\perp$ distribution is harder in the data than in the Monte Carlo. For instance, in the region $p_\perp > 1.25$ GeV/c, we have the following ratios : $N_{data}/N_{MC} = 1.08 \pm 0.01_{stat}$ for the charged tracks spectrum dominated by pions, and $1.25 \pm 0.04_{stat}$ for the $\pi^\pm$ coming from K^0_s decays, indicating that the high part of the $p_\perp$ distribution is not well simulated for background events. Note however that there is an excellent agreement for

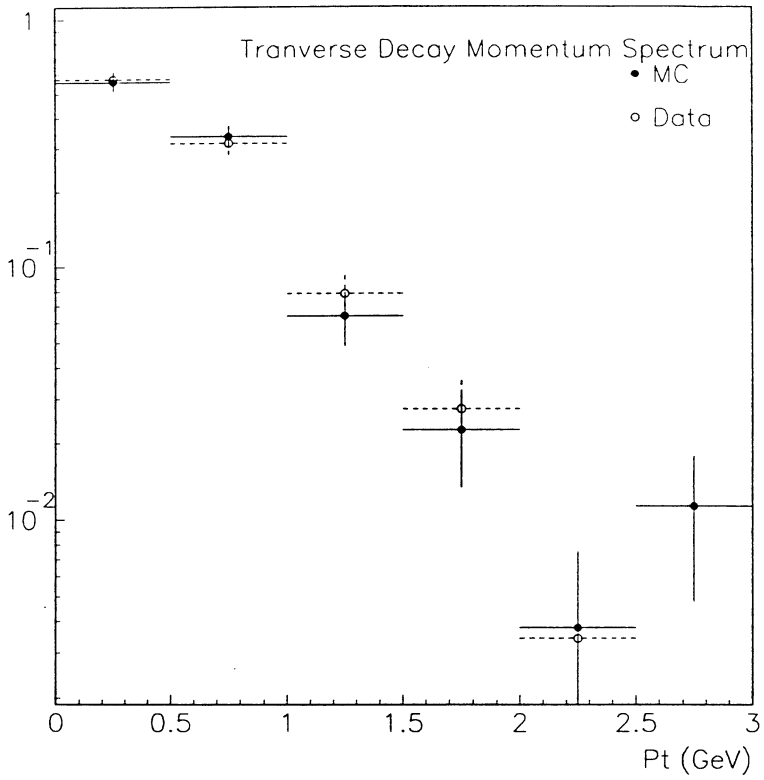

Figure 5: Transverse momentum distribution for the muon candidates in hadronic events with $|d_0| > 0.2$ cm. Comparison between '92 data (points) and '92 Monte Carlo (histogram) normalized to the same area.

the p distributions.

The list of the systematic errors on $R_b^{(1)}$ is given in table 5. For a more detailed description of the other sources of systematic errors, we refer to [3] and [5].

Finally, we obtain the following result :

$$R_b^{(1)} = 0.2230 \pm 0.0048_{stat.} \pm 0.0060_{syst.}$$

with

$$\Delta R_b^{(1)}(syst.) = 0.0028_{corel} \pm 0.0039_{charm} \pm 0.0035_{other}$$

where the contribution called *other* is dominated by the uncertainty on the background contamination in the muon sample.

The statistical accuracy on $R_b^{(1)}$ is limited by the opposite side dilepton sample and the systematic error by the fact that we have to extract the light quark contribution from the simulation. Finally, we remark that with the '93 data, we will be able to improve this measurement (in reducing the systematic error) by using a harder $p_\perp$ cut (of the order of 1.50 GeV/c).

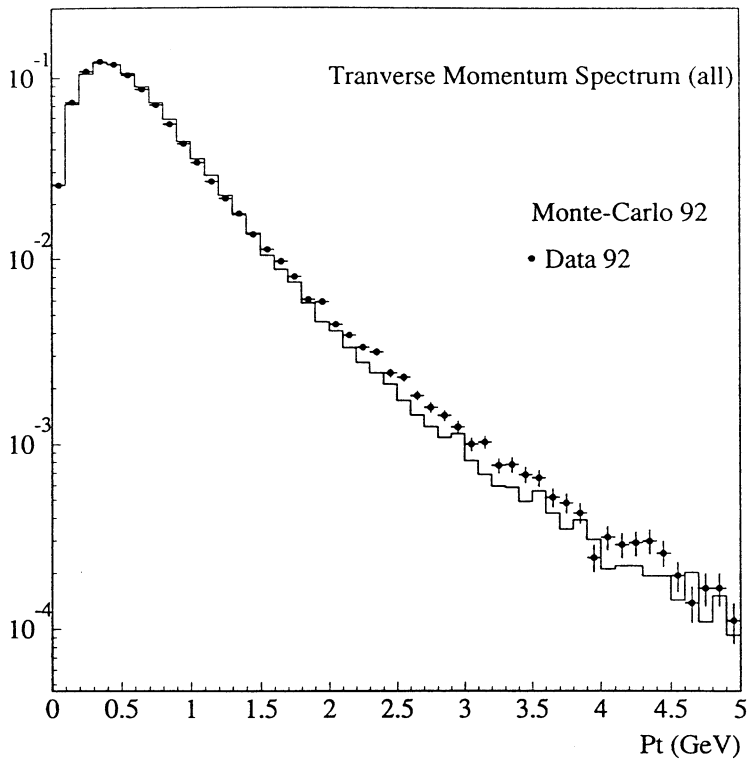

Figure 6: Transverse momentum distribution for the charged tracks with $p > 3$ GeV/c in hadronic Z events. Comparison between '92 data (points) and '92 Monte Carlo (histogram) normalized to the same number of tracks.

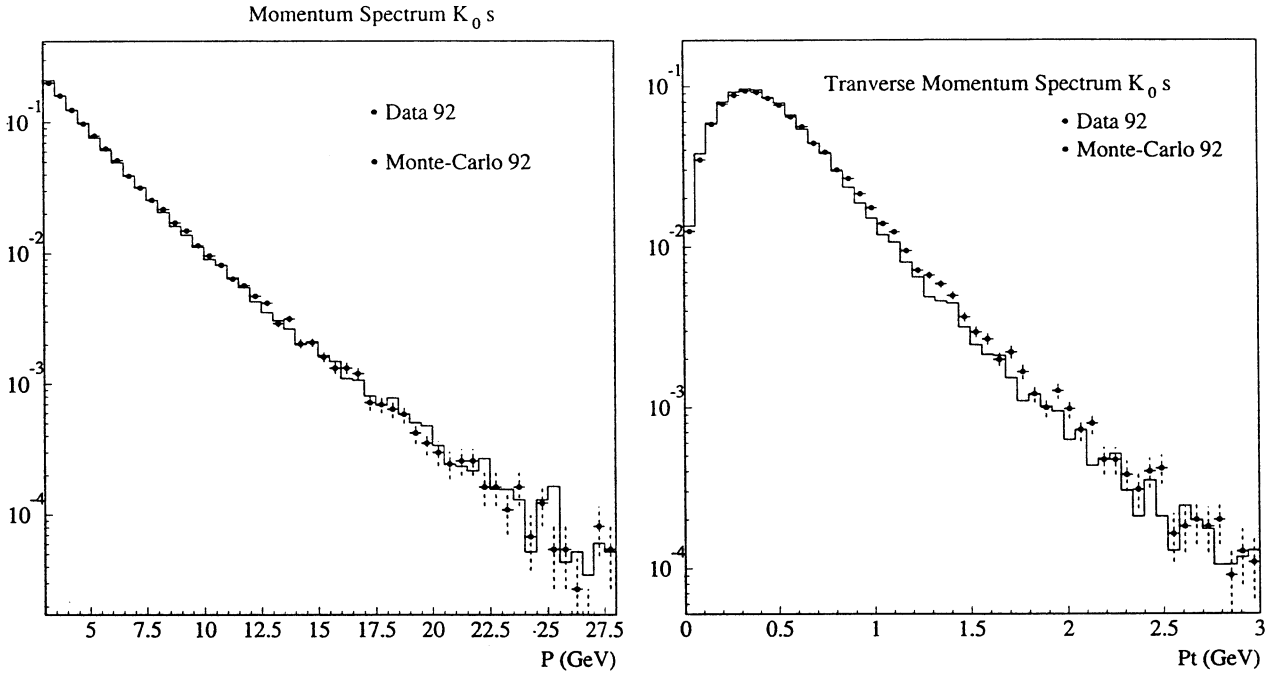

Figure 7: Momentum and transverse momentum distribution of the $\pi^{\pm}$ candidates coming from K_s^0 decays. Comparison between '92 data (points) and '92 Monte Carlo (histogram) normalized to the same number of tracks.

Source	Variation	$\Delta R_b^{(1)}$ (%)		
		$p_\perp \geq$ 1.00	$p_\perp \geq$ 1.25	$p_\perp \geq$ 1.50
Charm fragmentation ϵ_c	1σ	$\pm$ 0.09	$\pm$ 0.13	$\pm$ 0.07
$c \rightarrow l$ modelling	1σ	$\pm$ 0.06	$\pm$ 0.05	$\pm$ 0.04
$R_c.BR(c \rightarrow l)$	10 %	$\pm$ 0.58	$\pm$ 0.36	$\pm$ 0.25
Leptons id efficiencies	3 %	$\pm$ 0.19	$\pm$ 0.12	$\pm$ 0.05
Electron misid.	10 %	$\pm$ 0.09	$\pm$ 0.02	$\pm$ 0.00
Conversions	10 %	$\pm$ 0.08	$\pm$ 0.01	$\pm$ 0.00
Punch through and decays	20-10 %	$\pm$ 0.60	$\pm$ 0.27	$\pm$ 0.20
Monte Carlo statistics	1σ	$\pm$ 0.16	$\pm$ 0.16	$\pm$ 0.16
$C = \frac{\epsilon_{b\bar{b}}}{\epsilon_b^2}$	1σ	$\pm$ 0.28	$\pm$ 0.28	$\pm$ 0.28
Selection correction C_b	1σ	$\pm$ 0.09	$\pm$ 0.09	$\pm$ 0.09
Total		$\pm$ 0.87	$\pm$ 0.59	$\pm$ 0.47

Table 5: Systematic uncertainties on $R_b^{(1)}$ for different $p_\perp$ cuts

3 Method (2) : Event shape and high $p_\perp$ lepton tag

Compared to the method (1), the aim is to reduce the statistical error on R_b by using all the hadronic events, and to determine the tagging efficiency ϵ_{udsc} of the light quarks directly from the data.

3.1 Principle of the method

This method uses two samples of single and double tagged hadronic events and a calibration sample which is mainly used to extract ϵ_b. The tagging of the hadronic events is done by using a Neural Network technique which combines in an optimal way the informations provided by nine event shape variables based on p and $p_\perp$ of the tracks of each hemisphere. All the details on the optimisation of the Neural Network and on the choice of the input variables can be found in [9] and [10]. The shape of the nine input variables and of the Neural Network output (noted RN in the following) are shown on figures 8, 9 and 10. Furthermore, the figure 11 shows that the shape of the Neural Network output agrees well between the different years of data taking.

From the three samples :

1. Single tagged hadronic sample N_{st} : events in which at least one hemisphere satisfies the cut on the Neural Network output,

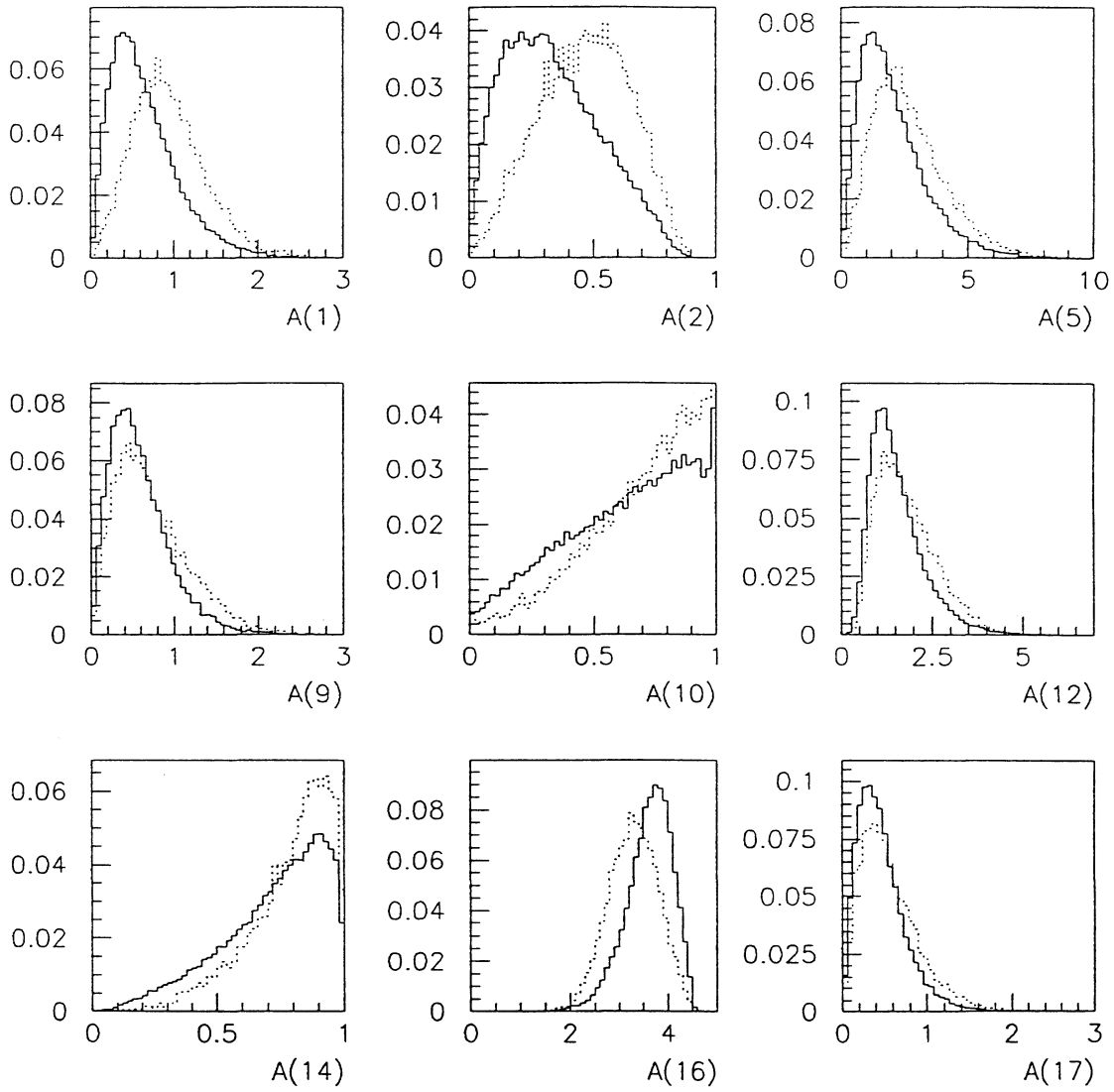

Figure 8: Distribution of the nine event shape variables used as input of the Neural Network. Comparison between $b\bar{b}$ (doted line) and *udsc* (solid line) events normalized to the same area.

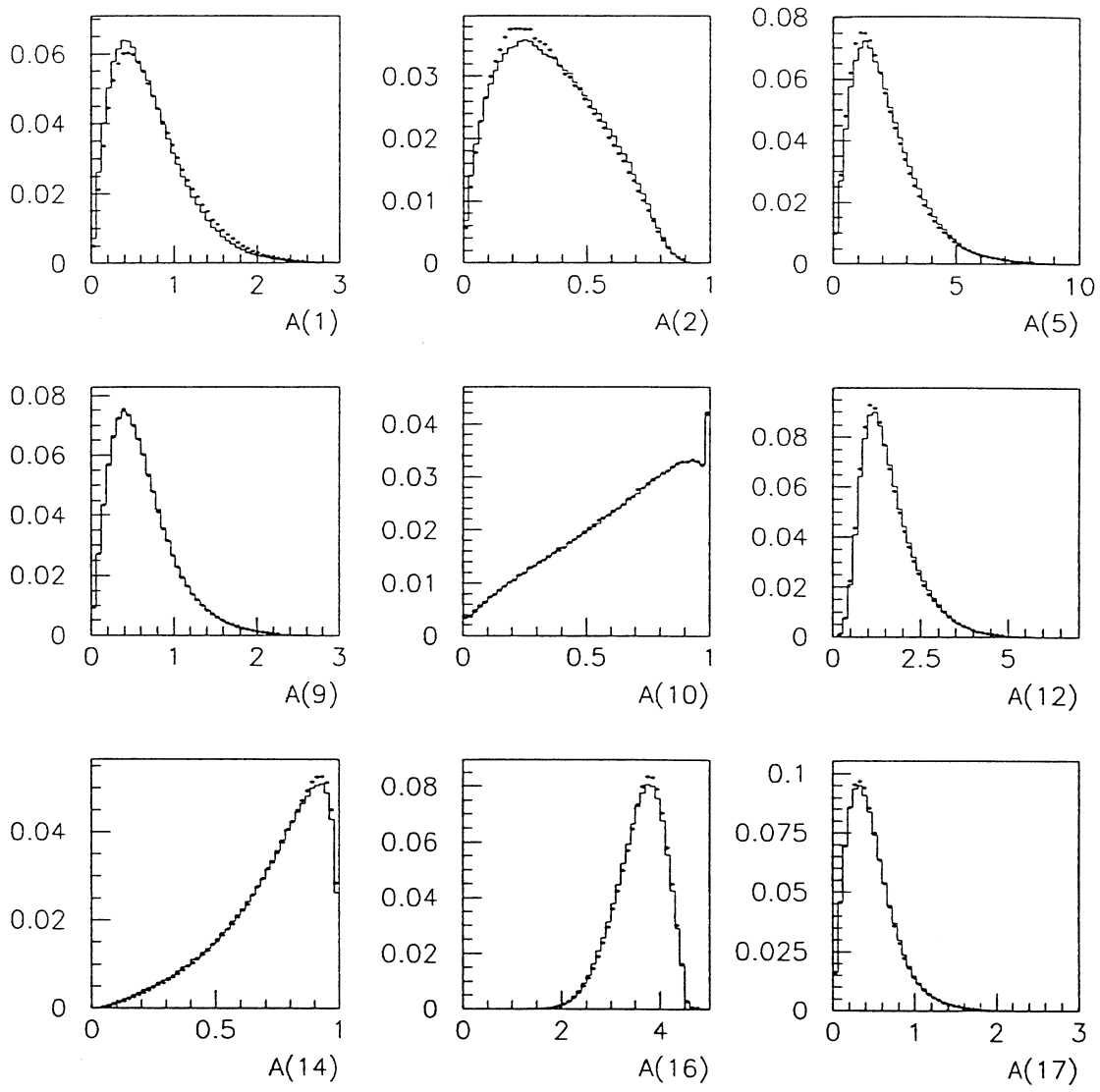

Figure 9: Distribution of the nine event shape variables used as input of the Neural Network. Comparison between simulated events (histogram) and data events (points).

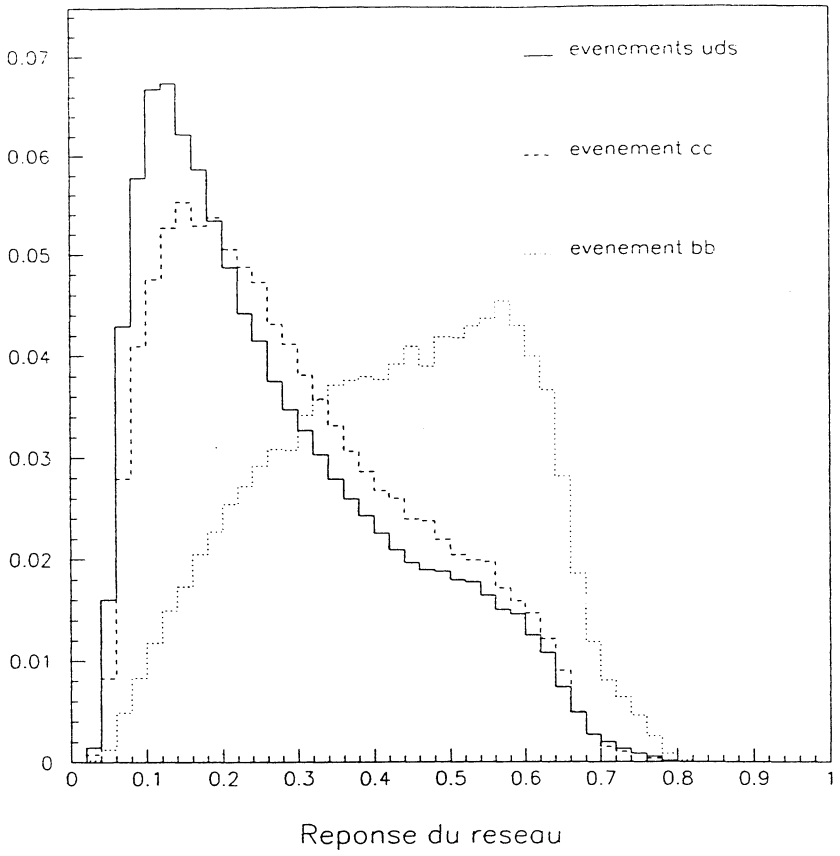

Figure 10: Neural Net. output for $b\bar{b}$ (dotted line), $c\bar{c}$ (dashed line) and *uds* (solid line) events. The three contributions are normalized to the same area.

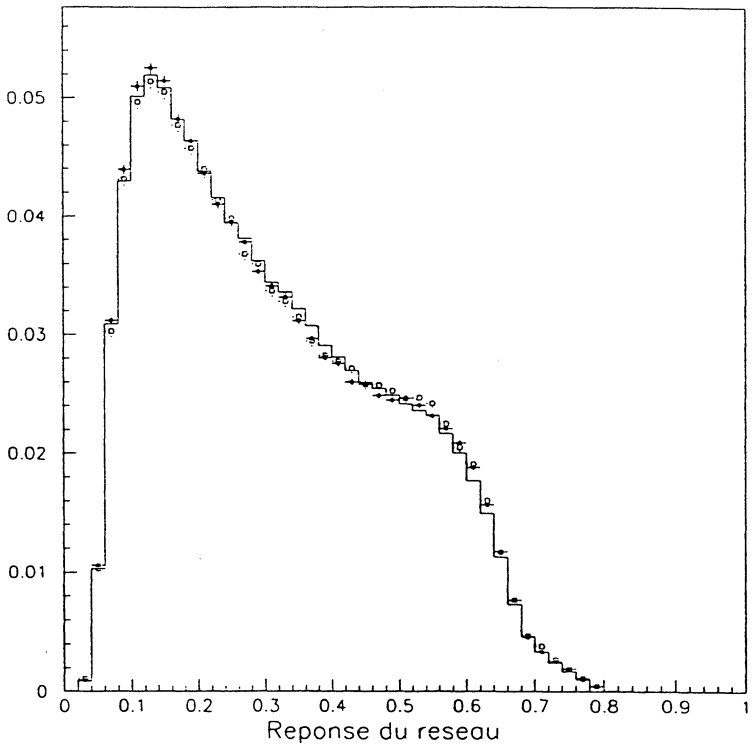

Figure 11: Comparison of the Neural Network output between '90 data (histogram), '91 data (squares) and '92 data (points).

2. Double tagged hadronic sample N_{dt} : events in which both hemispheres satisfy the cut on the Neural Network output,

3. Single tagged high $p_\perp$ leptons N^l_{st} : events tagged by a high $p_\perp$ lepton on one side, and by the event shape discriminator on the other side,

$R_b^{(2)}$ is derived by solving the following system of three equations with three unknowns f_b, ϵ_b and ϵ_{udsc} :

$$\left\{ \begin{array}{lcl} \frac{N_{st}}{2\,N_{had}} & = & f_b\,\varepsilon_b + (1-f_b)\,\varepsilon_{udsc} \\ \frac{N_{dt}}{N_{had}} & = & f_b\,\varepsilon_b^2\,(1+C_b^{dt}) + (1-f_b)\,\varepsilon_{udsc}^2(1+C_{udsc}^{dt}+K_{udsc}^{dt}) \\ \frac{N^l_{st}}{N_{lep}} & = & f_b^l\,\varepsilon_b\,(1+C_b^l) + (1-f_b^l)\,\varepsilon_{udsc}\,(1+C_{udsc}^l+K_{udsc}^l) \end{array} \right. \qquad (2)$$

• $R_b^{(2)} = C_b f_b$ where f_b is the fraction of $Z \rightarrow b\bar{b}$ events in the selected hadronic sample and C_b a correction factor which takes into account for the difference in acceptance between $b\bar{b}$ events and light quark events. This factor has been estimated by Monte Carlo and is equal to : $C_b = 0.987 \pm 0.002(stat.) \pm 0.002(syst.)$. The main contribution in this factor comes from the requirement of at least four tracks in the most energetic jet of each hemisphere (this is mandatory to correctly defined some imput variables). The first error is due to the limited Monte Carlo statistics and the second comes from the uncertainty on the charged tracks multiplicity in the b-hadron decays which can affect the previous cut.

• f_b^l is the hemisphere b-purity in the high $p_\perp$ lepton sample of the third equation and is determined for each year of data taking by the multi-lepton global fit [3]. With the '90, '91 and '92 data, we obtain : $f_b^l = 0.8814 \pm 0.0030_{stat.} \pm 0.0052_{syst.}$. Note that this is the average value for electrons and muons. This quantity will be discussed in more details in section 3.3.

• C_b^{dt} and C_{udsc}^{dt} are correction factors taken from the simulation, which take into account the fact that the two hemisphere taggings can be correlated by QCD effects and kinematical constraints. They are defined by the relation :

$$C_i^{dt} = \frac{\epsilon_i^{dt} - \epsilon_i^2}{\epsilon_i^2} \quad with \quad i = b,\ c,\ uds$$

where ϵ^{dt} is the probability that both hemispheres of an event satisfy a given cut on the Neural Net. output.

• C_b^l and C_{udsc}^l are correction factors taken from the simulation which take into account possible correlations between the two hemispheres due to the presence of a high $p_\perp$ lepton with missing energy carried out by a neutrino. They

are defined by the relation :

$$C_i^l = \frac{\varepsilon_i^l - \varepsilon_i}{\varepsilon_i} \quad \text{with} \quad i = b,\ c,\ uds$$

where ϵ^l is the probability to tag the hemisphere opposite to the high $p_\perp$ lepton.

• $K_{udsc}^{dt,l}$ are corrections accounting for a higher hemisphere tagging efficiency for $c\bar{c}$ events compared to uds events (see fig. 10). These two corrections can be written as :

$$K_{udsc}^{dt} = \frac{(1-f_c)f_c(\varepsilon_c - \varepsilon_{uds})^2}{\varepsilon_{udsc}^2}$$

$$K_{udsc}^{l} = \frac{(f_c^l - f_c)(\varepsilon_c - \varepsilon_{uds})}{\varepsilon_{udsc}}$$

where f_c and f_c^l are the fractions of $c\bar{c}$ events in the hadronic and high $p_\perp$ lepton samples respectively, which are determined by the global analysis of ref. [3]. One has : $f_c = 0.21 \pm 0.02$ and $f_c^l = 0.57 \pm 0.07$.

3.2 Results

A previous analysis has shown that the optimal cuts for the total error on $R_b^{(2)}$ are 0.3 for the Neural Net. output and 1.25 GeV/c for the lepton transverse momentum. Furthermore, since the results with '90 and '91 data have been published, we only concentrate in this note on the result obtained with '92 data.

The values of the 6 correction factors $C_{b,udsc}^{dt,l}$ and $K_{udsc}^{dt,l}$ used to solve the system 2 are given in table 6. The values of the tagging efficiencies ϵ_b and ϵ_{udsc}

Coefficient	Monte Carlo values
C_b^{dt}	0.001 ± 0.001
C_b^l	-0.001 ± 0.001
C_{udsc}^{dt}	0.033 ± 0.002
C_{udsc}^l	-0.001 ± 0.016
K_{udsc}^{dt}	0.005 ± 0.002
K_{udsc}^l	0.060 ± 0.015

Table 6: Values of the 6 correction coefficients for a Neural Net. cut at 0.3 and a cut on $p_\perp$ at 1.25 GeV/c.

estimated with the '92 data are shown on figure 12. The results obtained on $f_b^{(2)}$ for different cuts on the Neural Network output and on the $p_\perp$ of the leptons are summarized in tables 7 and 8 with '92 data and are illustrated on figure 13.

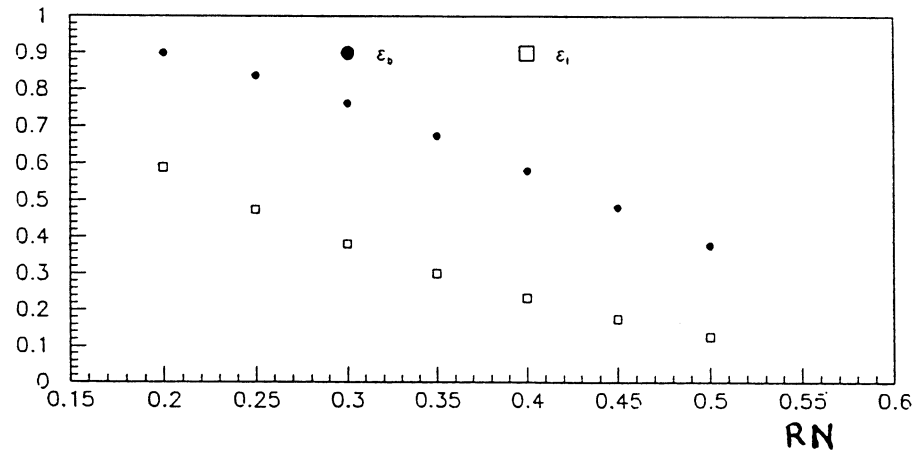

Figure 12: Values of ϵ_b and ϵ_{udsc} obtained with the '92 data as function of the cut applied on the Neural Net. output.

RN^{cut}	$f_b^{(2)}$ (%)	ϵ_b (%)	ϵ_{udsc} (%)
0.15	20.86 ± 1.52	95.28 ± 0.17	74.49 ± 0.49
0.20	22.68 ± 0.62	90.24 ± 0.21	59.96 ± 0.30
0.25	22.97 ± 0.46	83.79 ± 0.25	48.09 ± 0.22
0.30	22.64 ± 0.42	76.35 ± 0.28	38.40 ± 0.18
0.35	22.46 ± 0.44	67.83 ± 0.30	30.32 ± 0.16
0.40	22.82 ± 0.48	58.08 ± 0.31	23.46 ± 0.15
0.45	22.59 ± 0.54	48.11 ± 0.31	17.78 ± 0.14
0.50	22.07 ± 0.61	37.89 ± 0.30	12.76 ± 0.13
0.55	22.09 ± 0.75	26.93 ± 0.27	8.09 ± 0.13
0.60	19.85 ± 1.06	15.85 ± 0.23	4.46 ± 0.12

Table 7: Value of $f_b^{(2)}$ for different cuts on the Neural Network output and $p_\perp \geq 1.25$ GeV/c, for the '92 data. Note that the values of $f_b^{(2)}$ are not corrected in this table by the acceptance factor C_b and by the subtraction of $Z \rightarrow \tau^+\tau^-$ events remaining after the CLAS 16 selection.

$p_\perp^{cut}$ (GeV/c)	$f_b^{(2)}$ (%)
0.75	22.63 ± 0.36
1.00	22.81 ± 0.39
1.25	22.64 ± 0.42
1.50	22.81 ± 0.46
1.75	23.04 ± 0.52

Table 8: Value of $f_b^{(2)}$ for different cuts on $p_\perp$ of the lepton and with a cut on the Neural Net. output at 0.3 for the '92 data. Same remarks as for the previous table.

They show that the determination of $f_b^{(2)}$ is stable within the uncorrelated error bars for this year of data taking. So, no problem can be seen at this level for '92 data compared to our published result.

Finally, the results obtained for the three years of data taking are given in table 9.

Year	f_b^l (%)	$R_b^{(2)}$ (%)	ϵ_b (%)	ϵ_{udsc} (%)
1990	88.40	22.70 ± 0.93	77.06 ± 0.63	38.31 ± 0.41
1991	88.10	22.70 ± 0.67	75.98 ± 0.47	37.93 ± 0.30
1992	88.10	22.60 ± 0.42	76.35 ± 0.28	38.40 ± 0.18
1990+1991+1992	88.14	22.64 ± 0.33	76.09 ± 0.22	38.11 ± 0.15

Table 9: Determination of $R_b^{(2)}$, ϵ_b and ϵ_{udsc} with '90, '91 and '92 data. Note that the results have been obtained with the same set of the 6 correction coefficients and for the cuts : $RN^{cut} = 0.3$ and $p_\perp^{cut} = 1.25$ GeV/c.

3.3 Systematic errors

The only point which will be discussed in this note is the determination of the hemisphere b purity f_b^l in the lepton sample of the third equation of the system 2. For the other points and for all the cross checks which have been done, we refer to the publication and to the previous ALEPH note.

Let us just recall briefly how this purity is determined from the data.

f_b^l can be written as : $f_b^l = N_b^l/(N_b^l + N_c^l + N_{uds}^l)$ where N_b^l, N_c^l and N_{uds}^l are the number of high $p_\perp$ lepton candidates from $b\bar{b}$, $c\bar{c}$ and uds events. The contributions from $Z \rightarrow b\bar{b}$ and $Z \rightarrow c\bar{c}$ events are experimentally determined on the basis of the global multilepton fit to the p and $p_\perp$ spectra of single and dilepton events, extracting R_b, R_c, $BR(b \rightarrow l)$, $BR(b \rightarrow c \rightarrow l)$ and the b and c

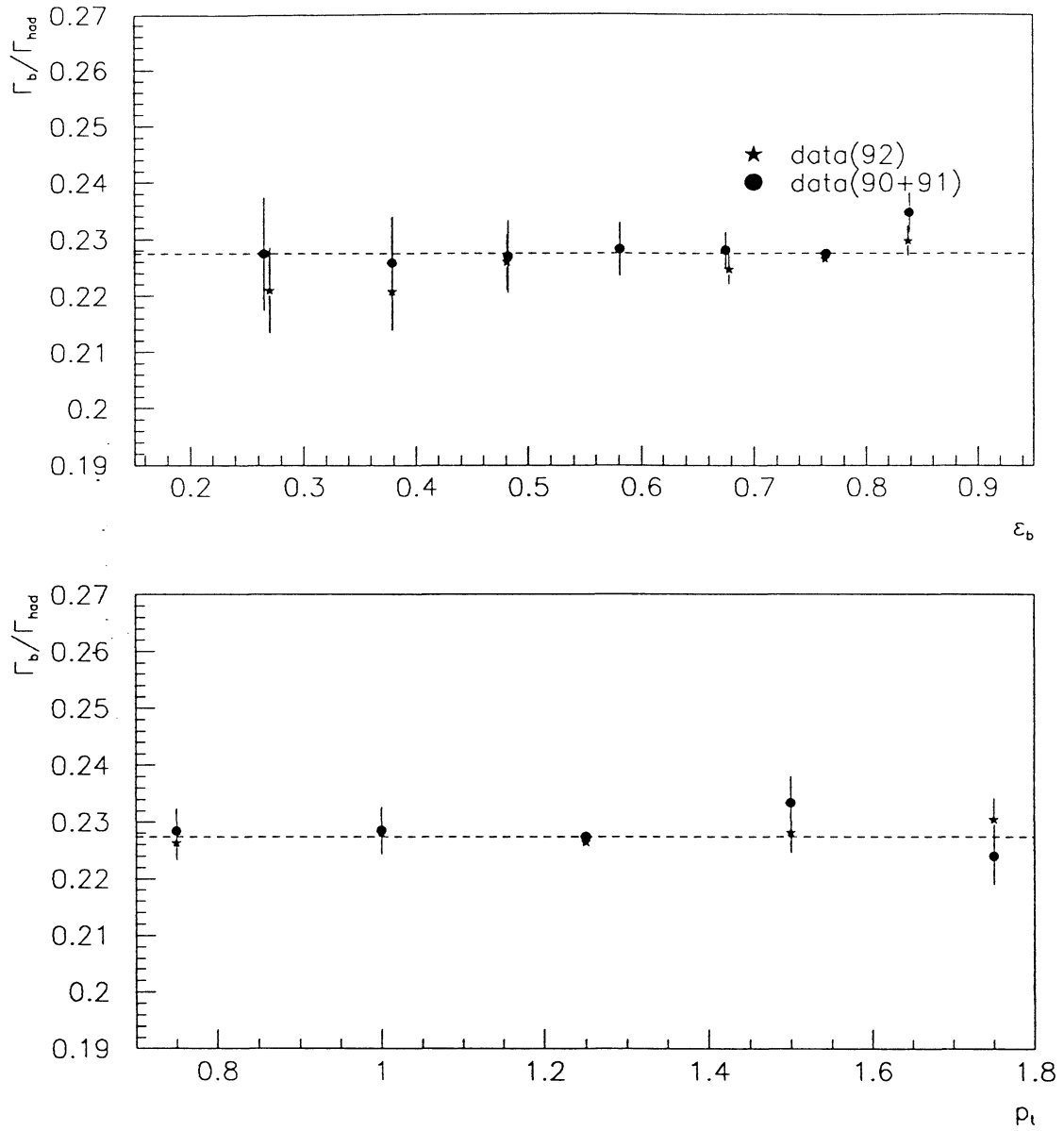

Figure 13: Values of $f_b^{(2)}$ obtained with the '90+'91 data (points) and with the '92 data (stars): a) for different cuts on the Neural Net. output and with $p_\perp^{cut} = 1.25$ GeV/c, b) for different cuts on $p_\perp$ and with $RN^{cut} = 0.3$. The points with dashed error bars are those with the standard cuts and these error bars show the total statistical error. The points for the other cuts have statistical errors for the difference relative to the standard cut points (uncorrelated errors).

fragmentation parameters [3]. Once these parameters are known with the full (p, $p_\perp$) analysis, the contribution of the various lepton sources can then be computed in any restricted $p_\perp$ region and f_b^l determined.

The sample composition determined by the global multilepton analysis applied to the '91 data is given in table 10 for the region $p_\perp > 1.25$ GeV/c.

Event type	e	μ	total
Prompt b	91.1%	82.5%	85.8%
$c \rightarrow l^+$	5.6%	5.8%	5.7%
$\text{Background}_\text{b}$	0.9%	3.2%	2.3%
$\text{Background}_\text{c}$	0.4%	1.8%	1.2%
$\text{Background}_\text{uds}$	2.0%	6.7%	5.0%

Table 10: Sample composition for electrons and muons and for the total sample, with $p > 3$ GeV/c and $p_\perp > 1.25$ GeV/c. These fractions are determined by the global multilepton analysis. Note that for the electrons, the background is composed of photon conversions (60%) and of misidentified hadrons (40%) while in the muon case, it is composed of punch through (60%) and decays (40%).

As for method (1), the two important points are the control of the background in the high $p_\perp$ region and the modelling of the prompt lepton momentum spectra.

– The first point has been already discussed in section 2.3 and should also be studied with care since the uncertainty on the background can have significant effects on f_b^l. For the muon study, only the determination of the misidentification probabilities from the data has been performed, but the study of the $p_\perp$ distribution has to be done.

– For the $b \rightarrow l$ transitions, all the publications based on the '90 and '91 data have used the ACCMM model and the ISGW model with 32% D^{**} (noted $ISGW^{**}$ in the following) optimised on the CLEO data. So, our error on f_b^l was estimated by taking half difference between the two models. To follow the prescriptions of the Heavy Flavour Electroweak Working group, we should also considered the ISGW model with its prediction of 11% D^{**} (noted ISGW in the following). Then, the central value of f_b^l has to be estimated with the ACCMM model and the error computed by using the ISGW and $ISGW^{**}$ models. Since the shape predicted by the ACCMM model lies between the ISGW and $ISGW^{**}$ distributions (see figure 14), the net effect will be to multiply by a factor two the previous estimate of the systematic error on f_b^l due to the $b \rightarrow l$ modelling. Note however, that this ISGW model does not correctly reproduce the lepton momentum distribution of CLEO. So, we believe that this estimate of the systematic error is rather pessimistic.

– For the $c \rightarrow l$ transitions, we should also follow the procedure used for the method (1).

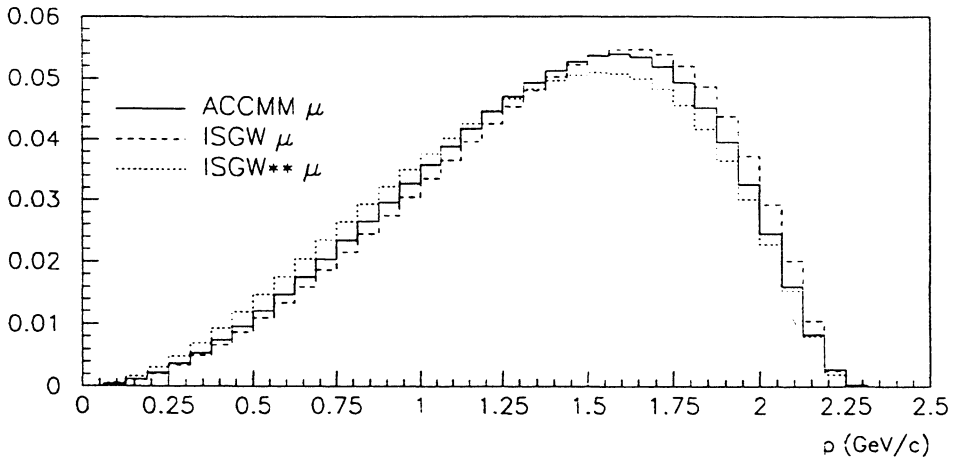

Figure 14: Momentum spectrum of the lepton in the rest frame of the B meson for $b \to l$ decays, for the ACCMM, ISGW and $ISGW^{**}$ models.

– For the $b \to c \to l$ transitions, the procedure is to combined the measured $B \to D$ spectrum from CLEO [12] (the error on this distribution is negligible) and to use the model described previously for the $D \to l$ part. In this approach, the $b \to c \to l$ and $c \to l$ models are correlated through the $c \to l$ decays and they are varied simultaneously. So, we can expect to decrease our error due to these two contributions compared to the table 11 where the two contributions are treated as independent.

Finally, we can note that the new $c \to l$ model is harder than the JETSET prediction while the $B \to D$ spectrum from CLEO is softer than the distribution predicted by JETSET.

The systematic errors on f_b^l are summarized in table 11 for a $p_\perp$ cut at 1.25 GeV/c. All the improvements from the Electroweak working group are not yet incorporated in this table. The effect should be a small increase of the systematic error of f_b^l.

The determination of the b-purity has been done for the '90 and '91 data. For 1992, we take the same value of f_b^l as for 1991 since the official results of the global multilepton analysis are not yet available for this year.

Finally, we obtain :

$f_b^l = 0.8814 \pm 0.0030_{stat.} \pm 0.0052_{syst.}$.

The systematic errors on $R_b^{(2)}$ are summarized in table 12.

Finally, we obtain by adding '90, '91 and '92 data :

$$R_b^{(2)} = 0.2264 \pm 0.0033_{stat.} \pm 0.0041_{syst.}$$

Source	Error	σf_b^l (%)
Statistical error of the fit	$\pm 1\sigma$	± 0.30
$b \to l$ model.	$Altarelli/ISGW^{**}$	± 0.25
$c \to l$ model.	Data ($\pm 1\sigma$)	± 0.06
$b \to c \to l$ model.	Data ($\pm 1\sigma$)	± 0.35
Electron Id. efficiency	$\pm 3\%$	± 0.02
Muon Id. efficiency	$\pm 3\%$	± 0.03
Photon conversions	$\pm 10\%$	± 0.14
Electron misid.	$\pm 10\%$	± 0.07
$\mu - decay$	$\pm 10\%$	± 0.21
Punch-through	$\pm 20\%$	± 0.13
Systematic error		± 0.52
Stat. + syst. error		± 0.60

Table 11: Sources of systematic errors and their contributions to the error on f_b^l. Note that the $c \to l$ and $b \to c \to l$ contributions are varied independently.

Source	Effect on $R_b^{(2)}$ (%)
f_b^l	± 0.30
C_b^{dt}	± 0.10
C_{uds}^{dt}	± 0.13
C_b^l	± 0.10
C_{uds}^l	± 0.10
Charm fragmentation	± 0.08
f_c	± 0.00
f_c^l	± 0.05
Beauty fragmentation	± 0.06
$BR(b \to l\nu X)$	± 0.03
Background	± 0.01
Geometrical effects	± 0.07
Acceptance factor C_b	± 0.06
Total	± 0.41

Table 12: List of the contributions to the systematic error on $R_b^{(2)}$.

with

$$\Delta R_b^{(2)}{}_{syst.} = 0.0022_{corel} \pm 0.0009_{charm} \pm 0.0030_{f_b^l} \pm 0.0011_{other}$$

4 Method (3) : Event shape and lifetime tag

The sample of high $p_\perp$ leptons in the third equation of the method (2) limits the statistical accuracy on $R_b^{(2)}$ but also its systematic error through the uncertainty on the $b\bar{b}$ purity f_b^l. So, we have replaced in the third equation of the system 2 the high $p_\perp$ lepton tag by a cut on the vertex variable Probhemi [13].

4.1 Principle of the method

We obtain the following new system where f_b^l, $C_{b,udsc}^l$ and K_{udsc}^l are replaced respectively by f_b^{vdet}, $C_{b,udsc}^{vdet}$ and K_{udsc}^{vdet} :

$$\left\{ \begin{array}{lcl} \frac{N_{st}}{2\,N_{had}} & = & f_b\,\varepsilon_b + (1-f_b)\,\varepsilon_{udsc} \\ \frac{N_{dt}}{N_{had}} & = & f_b\,\varepsilon_b^2\,(1+C_b^{dt}) + (1-f_b)\,\varepsilon_{udsc}^2(1+C_{udsc}^{dt}+K_{udsc}^{dt}) \\ \frac{N_{st}^{vdet}}{N_{vdet}} & = & f_b^{vdet}\,\varepsilon_b\,(1+C_b^{vdet}) + (1-f_b^{vdet})\,\varepsilon_{udsc}\,(1+C_{udsc}^{vdet}+K_{udsc}^{vdet}) \end{array} \right. \quad (3)$$

– f_b^{vdet} is the b-purity in the hadronic sample for a given cut on Probhemi. It is determined by the analysis described in [13].

– C_b^{vdet} and C_{udsc}^{vdet} are correction factors taken from the simulation which take into account possible correlations between the event shape and the lifetime tag. They are defined by the relation :

$$C_i^{vdet} = \frac{\epsilon_i^{vdet} - \epsilon_i}{\epsilon_i} \quad \text{with} \quad i = b,\ c,\ uds$$

where ϵ^{vdet} is the probability to tag one hemisphere by the Neural Network as soon as the opposite hemisphere has been tagged by Probhemi. Since the two tags are independent, we expect very small values for these coefficients.

– K_{udsc}^{vdet} is a correction factor accounting for a higher hemisphere tagging efficiency for $c\bar{c}$ events compared to *uds* events. This coefficient can be written as :

$$K_{udsc}^{vdet} = \frac{(f_c^{vdet} - f_c)(\epsilon_c - \epsilon_{uds})}{\epsilon_{udsc}}$$

where f_c^{vdet} is the fraction of $c\bar{c}$ events in a sample of *udsc* hadronic events tagged by Probhemi. Its value is determined by Monte Carlo.

4.2 Results

• *Determination of* f_b^{vdet} *and* f_c^{vdet}

– The b-purity f_b^{vdet} is given by the relation :

$$f_b^{vdet} = \frac{\epsilon_b^{vdet} R_b^{vdet}}{\epsilon_b^{vdet} R_b^{vdet} + \epsilon_{udsc}^{vdet}(1 - R_b^{vdet})}.$$

where $R_b^{vdet} = 0.2192 \pm 0.0037$ from the published lifetime analysis [13]. The value of the tagging efficiency, ϵ_b^{vdet} is also taken from the lifetime analysis of D. Brown et al. [13].

Since ϵ_{udsc}^{vdet} is mainly determined from the simulation, we have to minimize its contribution to f_b^{vdet} by using a very pure b sample in the third equation of the new system. We will choose in the following a cut on $\log(Probhemi)$ at -5.6 leading to a b purity of about 99%.

ϵ_{udsc}^{vdet} can be written as :

$$\epsilon_{udsc}^{vdet} = \frac{\epsilon_c^{vdet} R_c^{lept} + \epsilon_{uds}^{vdet}(1 - R_c^{lept} - R_b^{vdet})}{1 - R_b^{vdet}}$$

with $R_c^{lept} = 0.165 \pm 0.021$ taken from the multilepton fit. The value of R_b^{vdet} was obtained for a cut on $\log(Probhemi)$ at -4. For this cut, the relative uncertainties on ϵ_c^{vdet} and ϵ_{uds}^{vdet} are respectively 12.7% and 11%. Since we have chosen for our analysis a harder cut, we are more sensitive to statistical fluctuations and to possible distorsions of the momentum spectrum of $K^{\pm}$ to estimate ϵ_{uds}^{vdet}, and to rare charm meson decays with a high multiplicity (more than 5 prongs) for ϵ_c^{vdet}. So, we assign a relative uncertainty of $\pm 20\%$ for both ϵ_{uds}^{vdet} and ϵ_c^{vdet} and we obtain $\epsilon_{udsc}^{vdet} = (0.034 \pm 0.007)\%$. Finally, with $\epsilon_b^{vdet} = (12.78 \pm 0.10)\%$, we have : $f_b^{vdet} = 0.9905 \pm 0.0019$ for $\log(Probhemi) < -5.6$.

– The c-purity f_c^{vdet} in the non-b events of the third sample enters in the determination of the coefficient K_{udsc}^{vdet} and is estimated from the simulation. By using the relation :

$$f_c^{vdet} = \frac{\epsilon_c^{vdet} R_c^{lept}}{\epsilon_c^{vdet} R_c^{lept} + \epsilon_{uds}^{vdet}(1 - R_b^{vdet} - R_c^{lept})}$$

and with the values $\epsilon_c^{vdet} = (0.125 \pm 0.025)\%$ and $\epsilon_{uds}^{vdet} = (0.0098 \pm 0.0020)\%$, we obtain : $f_c^{vdet} = 0.78 \pm 0.07_{MC\ stat} \pm 0.05_{syst}$ where the dominant contributions to the systematic error come from the uncertainties on R_c^{lept}, ϵ_c^{vdet} and ϵ_{uds}^{vdet}.

• *Optimisation of the cuts*

To determine $R_b^{(3)}$, we have used 575,250 hadronic events selected in 1992. The tables 13 and 14 give the values of $f_b^{(3)}$ obtained for different cuts on the Neural Net. output and on $\log(Probhemi)$. The best cut on RN is the same as

for the method (2), i.e. $RN > 0.3$. The cut on $\log(Probhemi)$ at -5.6 leads to a rather high statistical error on $f_b^{(3)}$ and a lower cut on $\log(Probhemi)$ would improve this error. However, the systematic error due to the uncertainty on f_b^{vdet} will strongly increase in this case : for instance, with a cut at -2.0, we have $f_b^{vdet} = (77.3 \pm 3.4)\%$ where the error comes from the relative uncertainty of 20% on ϵ_{udsc}^{vdet}, leading to an absolute error of $\pm 1.1\%$ on $R_b^{(3)}$.

RN^{cut}	$f_b^{(3)}$ (%)	ϵ_b (%)	ϵ_{udsc} (%)
0.24	22.34 ± 0.45	86.46 ± 0.22	50.41 ± 0.24
0.26	22.42 ± 0.43	83.45 ± 0.24	46.18 ± 0.22
0.28	21.80 ± 0.41	80.72 ± 0.26	42.45 ± 0.20
0.30	22.08 ± 0.40	77.45 ± 0.27	38.69 ± 0.19
0.32	22.10 ± 0.41	74.34 ± 0.28	35.15 ± 0.18
0.34	21.75 ± 0.41	70.93 ± 0.29	32.12 ± 0.17
0.36	21.77 ± 0.42	67.37 ± 0.30	29.08 ± 0.16
0.38	21.97 ± 0.44	63.37 ± 0.31	26.27 ± 0.15
0.40	21.90 ± 0.46	59.42 ± 0.31	23.27 ± 0.15

Table 13: Solutions of the system for a cut on $\log(Probhemi)$ at -5.6.

$\lvert\log(Probhemi)\rvert$	$f_b^{(3)}$ (%)	ϵ_b (%)	ϵ_{udsc} (%)
2.00	21.51 ± 0.26	77.92 ± 0.15	38.80 ± 0.16
3.20	21.58 ± 0.30	77.85 ± 0.16	38.78 ± 0.17
4.00	21.76 ± 0.32	77.72 ± 0.19	38.73 ± 0.17
5.60	22.08 ± 0.40	77.45 ± 0.27	38.69 ± 0.19
6.00	22.02 ± 0.43	77.50 ± 0.30	38.66 ± 0.19
6.40	22.10 ± 0.72	77.43 ± 0.33	38.13 ± 0.26

Table 14: Solutions of the system for a cut on the Neural Net. output at 0.3.

The 6 correction coefficients which enter in the system 3 are estimated with 690,000 fully simulated *udsc* events and with 414,000 $Z \rightarrow b\bar{b}$ events (see table 15). They are compatible with the values obtained in the method (2) except K_{udsc}^{vdet} which is larger than K_{udsc}^{l} because these coefficients are proportionnal to $\epsilon_c^{vdet} - \epsilon_c$ and to $\epsilon_c^{l} - \epsilon_c$ respectively. Their errors are determined in the same way as for the previous method.

The results obtained on $f_b^{(3)}$ for different cuts on the Neural Network output and on $\log(Probhemi)$ are illustrated on figures 15, and 16. They show that the determination of $f_b^{(3)}$ is stable within the errors bars.

Coefficient	Monte Carlo value
C_b^{dt}	0.0008 ± 0.0012
C_b^{vdet}	0.0019 ± 0.0018
C_{udsc}^{dt}	0.027 ± 0.0020
C_{udsc}^{vdet}	0.0005 ± 0.050
K_{udsc}^{dt}	0.0042 ± 0.002
K_{udsc}^{vdet}	0.088 ± 0.024

Table 15: Values of the 6 correction coefficients for a Neural Net. cut at 0.3 and a cut on $\log(Probhemi)$ at -5.6.

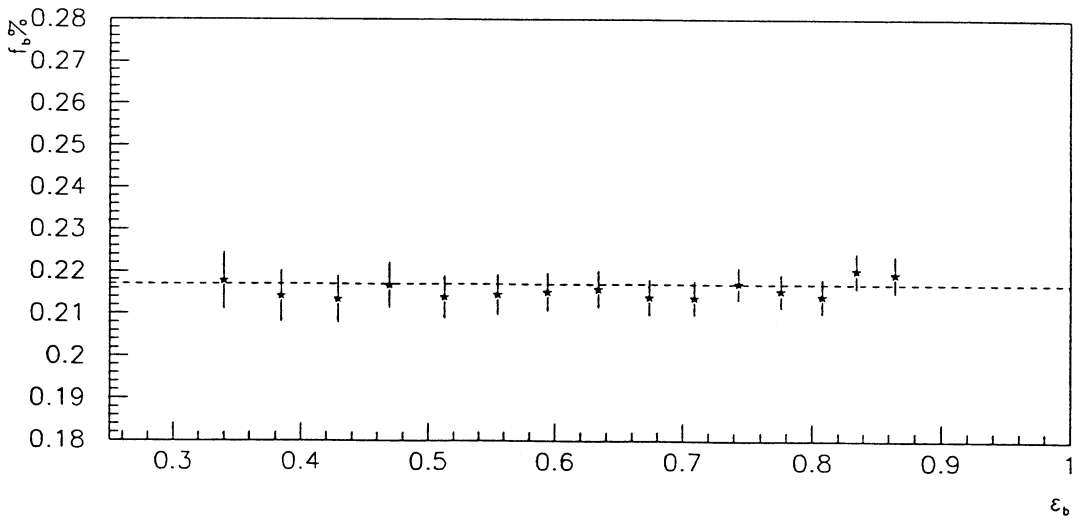

Figure 15: Values of $f_b^{(3)}$ obtained with the '92 data for different cuts on the Neural Net. output and with $\log(Probhemi) < -5.6$. Note that the statistical errors are correlated.

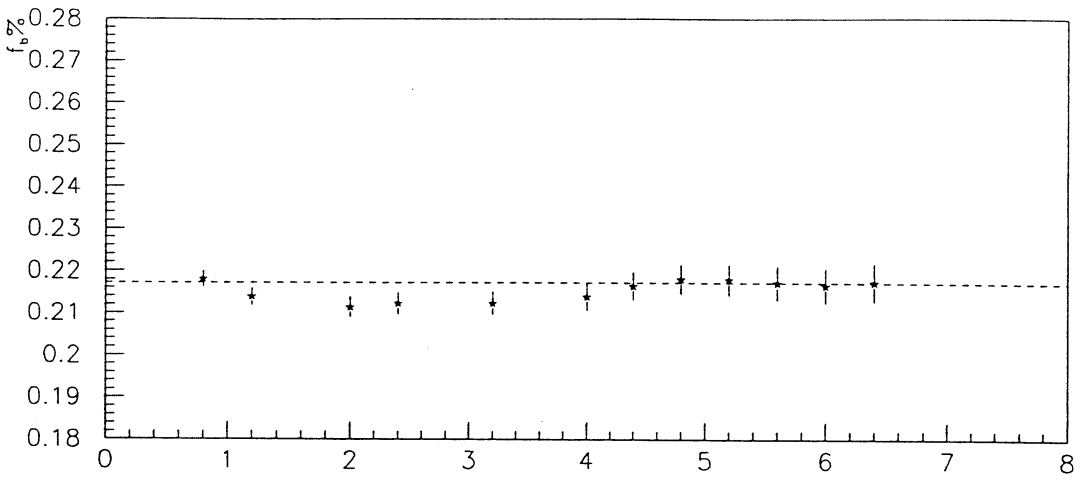

Figure 16: Values of $f_b^{(3)}$ obtained with the '92 data for different cuts on $\log(Probhemi)$ and with $RN^{cut} = 0.3$. Same remark as for the previous figure.

4.3 Systematic errors

The estimation of the systematic errors is done in the same way as for method (2). These errors are summarized in table 16. This leads to the following remarks :

– The error on $R_b^{(3)}$ due to f_b^{vdet} is smaller than the error on $R_b^{(2)}$ due to f_b^l by a factor 4.

– The error due to the charm fragmentation has increased by a factor 2.5. This comes from the fact that the two coefficients K_{udsc} which appear in the second and in the third equation of the systems produced anticorrelated effects on R_b. This cancellation does not occur for the method (3) since in this case, the b purity in the third equation is close to 100%, and so the coefficient K_{udsc}^{vdet} does not contribute to the systematic error of $R_b^{(3)}$.

Finally, our result is :

$$R_b^{(3)} = 0.2185 \pm 0.0040_{stat.} \pm 0.0034_{syst.}$$

with

$$\Delta R_b^{(3)}{}_{syst.} = 0.0025_{corel} \pm 0.0020_{charm} \pm 0.0008_{f_b^{vdet}} \pm 0.0009_{other}$$

5 Method (4) : Lifetime and high $p_\perp$ leptons

The second possibility to use the lifetime tag is to replace in method (2) the cut on the event shape tag by a cut on the Probhemi variable, the aim being to improve the discrimination power compared to the event shape tag.

Source	Effect on $R_b^{(3)}$ (%)
f_b^{vdet}	± 0.08
C_b^{dt}	± 0.11
C_{uds}^{dt}	± 0.16
C_b^{vdet}	± 0.16
C_{uds}^{vdet}	± 0.04
Charm fragmentation	± 0.20
f_c	± 0.02
f_c^{vdet}	± 0.01
Background	± 0.009
Geometrical effects	± 0.06
Acceptance factor C_b	± 0.06
Total contribution	± 0.34

Table 16: List of systematic errors on $R_b^{(3)}$.

5.1 Principle of the method

We obtain the following new system where the coefficients $C_{b,udsc}^{dt}$ and K_{udsc}^{dt} are replaced respectively by $C_{b,udsc}^{dt-vdet}$ and $K_{udsc}^{dt-vdet}$, and the tagging efficiencies $\epsilon_{b,udsc}$ by $\epsilon_{b,udsc}^{vdet}$:

$$\left\{ \begin{array}{lcll} \frac{N_{st}}{2\,N_{had}} & = & f_b\,\epsilon_b^{vdet} & + \; (1-f_b)\,\epsilon_{udsc}^{vdet} \\ \frac{N_{dt}}{N_{had}} & = & f_b\,(\epsilon_b^{vdet})^2\,(1+C_b^{dt-vdet}) & + \; (1-f_b)\,(\epsilon_{udsc}^{vdet})^2(1+C_{udsc}^{dt-vdet}+K_{udsc}^{dt-vdet}) \\ \frac{N_{st}^l}{N_l} & = & f_b^l\,\epsilon_b^{vdet}\,(1+C_b^l) & + \; (1-f_b^l)\,\epsilon_{udsc}^{vdet}\,(1+C_{udsc}^l+K_{udsc}^l) \end{array} \right. \quad (4)$$

5.2 Results

This analysis is also done with the '92 data. The tables 17 and 18 give the values of $f_b^{(4)}$ obtained for different cuts on $\log(Probhemi)$ and on $p_\perp$. From a statistical point of view, the best cut on $\log(Probhemi)$ is at -0.8. As for the method (2), the $p_\perp$ cut at 1.25 GeV/c will give the best overall error on $R_b^{(4)}$.

The values of the 6 correction coefficients which enter in this system are given in table 19 for $p_\perp > 1.25$ GeV/c and $\log(Probhemi) < -0.8$. The coefficients $C_{b,udsc}^{dt-vdet,l}$ are compatible with those obtained in the previous methods. On the other hand, the coefficients $K_{udsc}^{dt-vdet}$ and K_{udsc}^{l} are much bigger since they are proportional to the difference between the $c\bar{c}$ tagging efficiency, ϵ_c^{vdet}, and the

$\|\log(Probhemi)\|$	$f_b^{(4)}$ (%)	ϵ_b^{vdet} (%)	ϵ_{udsc}^{vdet} (%)
0.4	22.78 ± 0.46	86.42 ± 0.30	45.29 ± 0.25
0.8	22.61 ± 0.36	77.95 ± 0.34	23.94 ± 0.18
1.2	22.46 ± 0.37	70.36 ± 0.36	13.28 ± 0.17
1.6	22.98 ± 0.39	62.19 ± 0.37	7.43 ± 0.17
2.0	23.04 ± 0.41	54.71 ± 0.37	4.28 ± 0.16

Table 17: Solution of the system for several cuts on $\log(Probhemi)$ and with $p_\perp > 1.25$ GeV/c for the '92 data.

$p_\perp^{cut}$	$f_b^{(4)}$ (%)	ϵ_b^{vdet} (%)	ϵ_{udsc}^{vdet} (%)
1.00	23.00 ± 0.34	77.55 ± 0.31	23.78 ± 0.17
1.25	22.61 ± 0.36	77.95 ± 0.34	23.94 ± 0.18
1.50	22.64 ± 0.40	77.92 ± 0.38	23.93 ± 0.19
1.75	22.66 ± 0.45	77.90 ± 0.43	23.92 ± 0.21

Table 18: Solution of the system for several cuts on $p_\perp$ and with $|log(Probhemi)| > 0.8$ for the '92 data.

uds tagging efficiency, ϵ_{uds}^{vdet}, which are very different (for $\log(Probhemi) < -0.8$, we have : $\epsilon_c^{vdet} = 0.446$ and $\epsilon_{uds}^{vdet} = 0.185$).

Coefficient	Monte Carlo value
$C_b^{dt-vdet}$	0.0026 ± 0.0015
C_b^l	-0.00035 ± 0.0020
$C_{udsc}^{dt-vdet}$	0.0100 ± 0.0038
C_{udsc}^l	0.026 ± 0.024
$K_{udsc}^{dt-vdet}$	0.192 ± 0.019
K_{udsc}^l	0.380 ± 0.089

Table 19: Values of the 6 correction coefficients for a cut on $\log(Probhemi)$ at -0.8 and on $p_\perp$ at 1.25 GeV/c.

The results are illustrated on figures 17, and 18 for several cuts on $\log(Probhemi)$ and on $p_\perp$. They show that the determination of $f_b^{(4)}$ is stable within the errors bars.

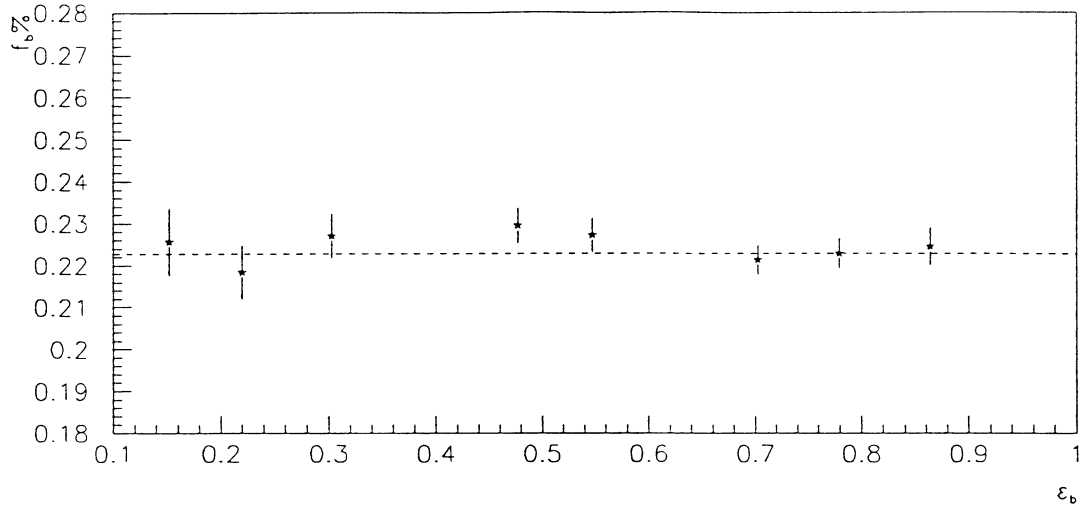

Figure 17: Values of $f_b^{(4)}$ obtained with the '92 data for different cuts on $\log(Probhemi) < -5.6$ and with $p_\perp > 1.25$ GeV/c. Note that the statistical errors are correlated.

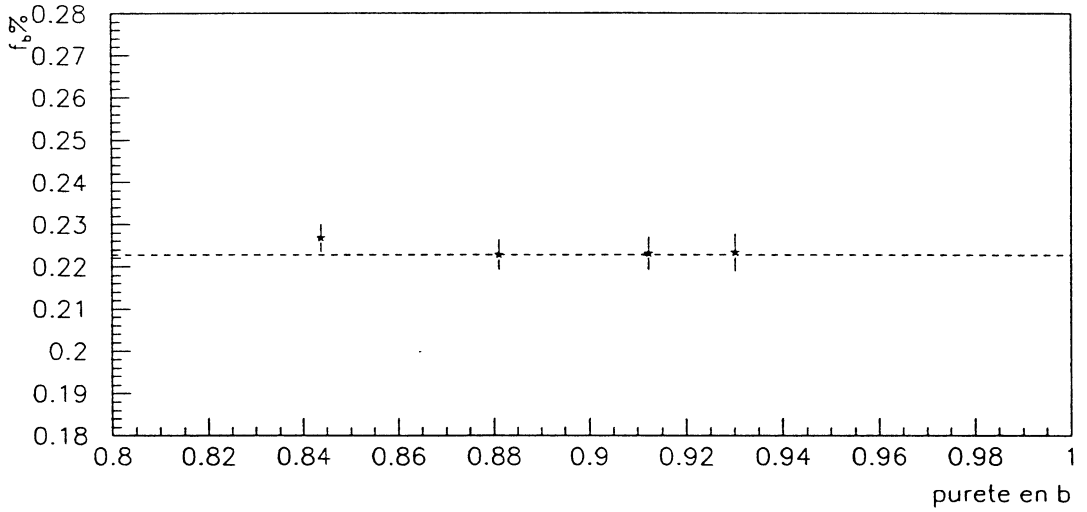

Figure 18: Values of $f_b^{(4)}$ obtained with the '92 data for different cuts on $p_\perp$ and with $\log(Probhemi) < -0.8$. Same remark as for the previous figure.

5.3 Systematic errors

These errors are summarized in table 20. From this table, we see that the large values of the $K_{udsc}^{dt-vdet,l}$ coefficients lead to important systematic errors on $R_b^{(4)}$ mainly due to the charm physics. So, this method will not contribute to improve our measurement of R_b.

Source	Effect on $R_b^{(4)}$ (%)
f_b^l	± 0.30
$C_b^{dt-vdet}$	± 0.08
$C_{udsc}^{dt-vdet}$	± 0.22
C_b^l	± 0.04
C_{udsc}^l	± 0.07
ϵ_{uds}^{vdet} and ϵ_c^{vdet}	± 0.20
f_c	± 0.29
f_c^l	± 0.22
Background	± 0.01
Geometrical effects	± 0.07
Acceptance factor C_b	± 0.07
Total contribution	± 0.57

Table 20: List of systematic errors on $R_b^{(4)}$.

Finally, we obtain with this method :

$$R_b^{(4)} = 0.2243 \pm 0.0036_{stat.} \pm 0.0057_{syst.}$$

with

$$\Delta R_b^{(4)}{}_{syst.} = 0.0025_{corel} \pm 0.0041_{charm} \pm 0.0030_{f_b^l} \pm 0.0010_{other}$$

6 Combined result of the four measurements

The results obtained on R_b by using high $p_\perp$ leptons, event shape variables and lifetime information to tag b quark events are summarized in table 21. All measurements are compatible within their uncorrelated errors.

The method used to combine these measurements is the "BLUE technique" described in [14].

According to this method, the combined measurement of R_b is taken to be the weighted mean of each of the individual measurements, $R_b = \sum_{i=1}^{4} \omega_i R_b^{(i)}$,

Method	Value of R_b (%)
(1)	$R_b^{(1)} = 22.30 \pm 0.48_{stat.} \pm 0.28_{corel} \pm 0.39_{charm} \pm 0.35_{other}$
(2)	$R_b^{(2)} = 22.64 \pm 0.33_{stat.} \pm 0.22_{corel} \pm 0.09_{charm} \pm 0.11_{other} \pm 0.30_{f_b^l}$
(3)	$R_b^{(3)} = 21.85 \pm 0.40_{stat.} \pm 0.25_{corel} \pm 0.20_{charm} \pm 0.09_{other} \pm 0.06_{f_b^{vdet}}$
(4)	$R_b^{(4)} = 22.43 \pm 0.36_{stat.} \pm 0.25_{corel} \pm 0.41_{charm} \pm 0.10_{other} \pm 0.30_{f_b^l}$

Table 21: Summary of the four results on R_b.

where the weights are determined by minimizing the total combined error σ^2 including both statistical and systematic contributions. σ^2 can be written as :

$$\sigma^2 = \sum_j^n \sum_i^4 (\omega_i \sigma_{ij})^2 + \sum_k^m (\sum_i^4 \omega_i \sigma_{ik})^2$$

where the first term corresponds to the n uncorrelated errors between the four measurements and the second one corresponds to the m fully correlated errors. The errors of each measurement are summarized in table 22.

• *Statistical errors*

– The statistical error for the method (1) comes from the opposite side dilepton sample (second equation of the system).

– The statistical error of the methods (2) and (4) is mainly due to the high $p_\perp$ lepton sample of the third equation of the systems. Since the contribution from the high $p_\perp$ dilepton events is small in this sample, we have considered this error uncorrelated with method (1). The statistical errors of methods (2) and (4) are considered as fully correlated even if the method (4) does not use '90 and '91 data.

– The statistical error of the method (3) mainly comes from the hadronic sample tagged with the vertex variable Probhemi. So, it is considered as fully uncorrelated with the others.

• *Systematic errors*

All these errors are taken to be fully correlated between the different measurements except the contribution due to the correction coefficients.

– The correction coefficient C of the method (1) only affects $b\bar{b}$ events and can be due to geometrical acceptance effects.

– The correction coefficients of methods (2) and (3) mainly affect light quark events and can be due to QCD effects or to kinematical constraints. Furthermore, they have been estimated with different Monte Carlo samples.

– The correction coefficients of method (4) are mainly due to the tagging by Probhemi.

Source	(1)	(2)	(3)	(4)	Combined
Statistical error ($\star$)	2.15	-	1.83	-	0.81
Statistical error	-	1.46	-	1.60	0.63
Correction coeff. ($\star$)	1.26	0.97	1.14	1.11	0.65
c–frag.	0.58	0.35	0.91	0.89	0.61
$c \rightarrow lmodel.$	0.05	-	-	-	0.01
f_c	1.61	-	0.09	1.28	0.32
f_c^l	-	0.22	-	0.98	0.09
f_c^{vdet}	-	-	0.05	-	0.02
lepton–Id	1.35	-	-	-	0.24
MC statistics	0.72	-	-	-	0.13
C_b factor	0.40	-	-	-	0.07
C_b factor	-	0.27	0.27	0.30	0.22
other	-	0.44	0.27	0.30	0.30
f_b^l	-	1.33	-	1.33	0.57
f_b^{vdet}	-	-	0.27	-	0.11
Syst. error	2.65	1.77	1.54	2.56	1.21
Syst. + stat. error	3.41	2.29	2.39	3.02	1.59

Table 22: List of fractional errors (in percent) on each individual measurement of R_b (first four columns) and on the combined result (final column). All the contributions are treated as fully correlated between the four results except for those labeled with a $\star$ which are considered as uncorrelated.

So, we have considered this systematic error as uncorrelated between the four methods.

The weights ω_i are then determined ; we obtain :

$$\omega_1 = 0.18 \quad \omega_2 = 0.43 \quad \omega_3 = 0.39 \quad \omega_4 = 0.$$

The method (4) doest not contribute to the weighted mean because its statistical error is considered as fully correlated with the method (1) and because this method has a large systematic error.

With these weights, we have our final result :

$$R_b = 0.2227 \pm 0.0023_{stat.} \pm 0.0027_{syst.}$$

$$\Delta R_{b\ syst.} = 0.0015_{corel} \pm 0.0015_{charm} \pm 0.0010_{other} \pm 0.0013_{f_b^l} \pm 0.0002_{f_b^{vdet}}$$

7 Future of these methods

At the end of LEP100, we should have about 4.10^6 hadronic Z per experiment. So, we can expect the following improvements :

- $\Delta R_b/R_b(stat.)$: $1.03\% \rightarrow 0.56\%$
- $\Delta R_b/R_b(charm\ frag.)$: $0.61\% \rightarrow 0.20\%$
- $\Delta R_b/R_b(f_b^l)$: $0.57\% \rightarrow 0.37\%$
- $\Delta R_b/R_b(syst.)$: $1.20\% \rightarrow 1.00\%$

The result on the charm fragmentation parameter $\epsilon_c(Peter)$ is completely dominated by the statistical error and only uses the '90 and '91 data. So, we can expect a significant improvement for this source of systematic error.

For the b-purity f_b^l which appears in the method (2), it seems reasonable to expect a decrease by a factor two on the uncertainties due to the $b \rightarrow l$, $c \rightarrow l$ and $b \rightarrow c \rightarrow l$ modelling since CLEO II will provide us improved informations on that. But it is clear that we have to better understand the shape of the $p_\perp$ distribution of the background in the muon sample if we want to improve significantly the error on f_b^l.

Concerning the correlation coefficients, it seems difficult for us to reduce their contribution to the error since they are taken from the simulation. We can perhaps imagine to determine these coefficients from the data in the b case by using a lifetime tag to have a very pure sample of $Z \rightarrow b\bar{b}$ events, but the problem seems more difficult for the *udsc* events.

So finally, we can expect to measure R_b at LEP100 with a relative accuracy of the order of 1.2% limited by the systematics.

This method mainly uses the large mass of the b quark, and then is for a large part uncorrelated with the pure lifetime method.

References

[1] D. BUSKULIC ET AL. (ALEPH COLL.), Phys Lett B 313 (1993) 535.

[2] F. SAADI, *Mesure de la Largeur Partielle de désintégration du boson Z en paire de quarks beaux par des méthodes de double étiquetage dans ALEPH* ; Thèse de l'Université Blaise Pascal - Clermont-Fd, Feb. 22 1994. PCCF T/94-03.

[3] D. BUSKULIC ET AL. (ALEPH COLL.), *Heavy Flavour Production and Decay with Prompt Lepton in the ALEPH Detector*, submitted to Z. Phys. C.

[4] J. LEFRANCOIS, EPS Conference on High Energy Physics, July 1993, Marseille, France.

[5] F. SAADI ET AL., *A measurement of* $\Gamma(Z \to b\bar{b})/\Gamma(Z \to hadrons)$ *using single and double tagged events with high* $p_\perp$ *leptons*, ALEPH Note 93-68.

[6] D. BUSKULIC ET AL. (ALEPH COLL.), Phys. Lett. B 313 (1993) 549.

[7] F. SAADI ET AL., *Measurement of the Partial Width of the Z into b Quark Pairs using a Neural Network classifier with Jet shape variables*, March 16 1993, ALEPH Note 93-61.

[8] THE LEP ELECTROWEAK WORKING GROUP, *A Consistent Treatment of Systematic Errors for LEP Electroweak Heavy Flavour Analyses - Draft 3.0* 15th Feb. 1994, LEPHF/94-01.

[9] P. HENRARD, *Test du Modèle Standard électrofaible par l'étude de la beauté avec ALEPH* ; Habilitation à diriger des recherches, Université Blaise Pascal - Clermont-Fd, Nov. 18 1992. PCCF T/92-13.

[10] B. BRANDEL ET AL., *Event Shape Variables and Multivariate Analyses : An Approach to b quark Production and Fragmentation*, ALEPH note 91-85.

[11] D. BUSKULIC ET AL. (ALEPH COLL.), *Heavy Quark Tagging with Leptons in the ALEPH Detector*, submitted to N.I.M.

[12] CLEO COLL., Phys Rev. D 45 (1992) 21.

[13] D. BROWN, *QFNDIP, a primary vertex finder*, ALEPH Note 92-47;
D. BROWN ET AL., *Tagging of b hadrons using track impact parameters*, ALEPH Note 92-135;
D. BROWN, M. FRANK, A. GREENE, G. REDLINGER, *A Measurement of* $\Gamma_{b\bar{b}}/\Gamma_{had}$ *using a Lifetime b-tag*, ALEPH Note 93-39;
D. BROWN, M. FRANK, A. GREENE, G. REDLINGER, *Addendum to the Measurement of* $\Gamma_{b\bar{b}}/\Gamma_{had}$ *using a Lifetime b-tag (ALEPH note 93-39)*, ALEPH Note 93-83.

[14] L. LYONS ET AL., NIM A 270 (1988) 110.